Proceedings of ASME Turbo Expo 2011
GT2011
June 6-10, 2011, Vancouver, British Columbia, Canada

GT2011-45090

EXPERIMENTAL AND NUMERICAL STUDY OF NO_X FORMATION FROM THE LEAN PREMIXED COMBUSTION OF CH_4 MIXED WITH CO_2 AND N_2

K. Boyd Fackler
Dept of Mechanical Engineering
University of Washington
Seattle, Washington 98105
Email: kboydf@u.washington.edu

Megan F. Karalus
Dept of Mechanical Engineering
University of Washington
Seattle, Washington 98105
Email: karalm2@u.washington.edu

Igor V. Novosselov
Dept of Mechanical Engineering
University of Washington
Seattle, Washington 98105
Email: ivn@u.washington.edu

John C. Kramlich
Dept of Mechanical Engineering
University of Washington
Seattle, Washington 98105
Email: kramlich@u.washington.edu

Philip C. Malte
Dept of Mechanical Engineering
University of Washington
Seattle, Washington 98105
Email: malte@u.washington.edu

ABSTRACT

This paper describes an experimental and numerical study of the emission of nitrogen oxides (NO_X) from the lean premixed (LPM) combustion of gaseous fuel alternatives to typical pipeline natural gas in a high intensity, single-jet stirred reactor (JSR). In this study, CH_4 is mixed with varying levels CO_2 and N_2. NO_X measurements are taken at a nominal combustion temperature of 1800 K, atmospheric pressure, and a reactor residence time of 3 ms. The experimental results show the following trends for NO_X emissions as a function of fuel dilution: (1) more NO_X is produced per kg of CH_4 consumed with the addition of a diluent, (2) the degree of increase in emission index is dependent on the chosen diluent; N_2 dilution increases NO_X production more effectively than equivalent CO_2 dilution. Chemical kinetic modelling suggests that NO_X production is less effective for the mixture diluted with CO_2 due to both a decrease in N_2 concentration and the ability of CO_2 to deplete the radicals taking part in NO_X formation chemistry.

In order to gain insight on flame structure within the JSR, three dimensional computational fluid dynamic (CFD) simulations are carried out for LPM CH_4 combustion. A global CH_4 combustion mechanism is used to model the chemistry. While it does not predict intermediate radicals, it does predict CH_4 and CO oxidation quite well. The CFD model illustrates the flowfield, temperature variation, and flame structure within the JSR. A 3-element chemical reactor network (CRN), including detailed chemistry, is constructed using insight from detailed spatial measurements of the reactor, the results of CFD simulations, and classical fluid dynamic correlations. GRI 3.0 is used in the CRN to model the NO_X emissions for all fuel blends. The experimental and modelling results are in good agreement and suggest the underlying chemical kinetic reasons for the trends.

1 Introduction

Lean-premixed (LPM) combustion technology is utilized in state of the art gas turbines to provide extremely efficient power generation with low emissions. Although there are many diffusion flame fired gas turbines still in place, LPM systems have been gaining popularity since the 1980's due to their inherent advantages in regards to emissions reduction. Traditionally, natural gas has been used almost exclusively in LPM combustion technology. While extensive research on natural gas-fueled LPM combustion has been reported, much less research has been con-

ducted on the use of alternatives to natural gas for LPM combustion devices. In the future, gas turbines will be run on a variety of fuel compositions ranging from syngases with high H_2 content to landfill and digester gas, which are mainly composed of CH_4, CO_2, and N_2. Alternative fuel blends will have a wide range of heating values, flame speeds, and chemical composition. It is important to study the behavior of these fuels under LPM conditions to maximize performance efficiency, while minimizing the overall emissions.

The use of landfill gas in LPM combustion systems is of interest for future gas turbine systems. Landfill gas is the product of the decomposition of municipal waste from landfills and waste-water treatment plants. Its composition varies depending on the feedstock; however, it is primarily composed of CH_4 and CO_2 with up to 15% N_2 and other trace compounds [1]. Qin et al. performed tests in a LPM stagnation flow experiment at atmospheric pressure and found that the addition of CO_2 to a LPM CH_4 flame increases the total NO_X emissions per mass of CH_4 consumed [2]. Recently some research has focussed on the effects of exhaust gas recirculation (EGR), where the oxidant stream is diluted with with products of combustion, namely: CO_2, N_2, and O_2 [3], [4], and [5]. Røkke et al. studied the effects of adding diluent to both LPM and diffusion flames at atmospheric pressure. In the LPM mode, they found that mixing was sufficient enough that it did not matter whether the diluent was injected into the fuel or oxidant stream. They also found that the addition of both N_2 and CO_2 decreased NO_X emissions; however, the flame temperature was not held constant [4]. ElKady et al. looked at the addition of 35% EGR to a LPM CH_4 flame at 10 atm and found that the EGR addition decreased NO_X emissions at constant flame temperature [3]. Li et al. studied the effect of varying both EGR percentage and pressure and found that at constant flame temperature, EGR increases NO_X formation at pressures below 5 atm, while EGR reduces NO_X emissions at pressures above 5 atm [5].

The main objective of this study is to evaluate NO_X formation as a function of CO_2 or N_2 dilution in LPM, constant temperature CH_4 combustion. Constant temperature experiments allow one to explore the influence of chemistry, while removing temperature as a variable. All of the experiments are conducted in a high intensity, single-jet, stirred reactor (JSR). The JSR has two distinct reaction zones much like the gas turbine combustor: a turbulent flame zone that is positioned right around the jet, followed by a post flame zone characterized by super-equilibrium free radical concentrations. Previous studies have shown that NO_X data taken from the JSR are comparable to data taken from actual gas turbine combustors operating at the same pressure and temperature [6]. Thus, the JSR is a useful experimental tool for performing kinetic studies on fuel mixtures that could be burned in a gas turbine.

First the experimental setup is briefly explained, followed by a presentation of the experimental results. The results of three dimensional CFD simulations are presented, which give insight to the flowfield, temperature distribution, and chemical composition of the reactor operating on CH_4. With the aid of the CFD results, a chemical reactor network is developed for the JSR. Its construction and layout are outlined and the model results are compared to experimental data.

2 Experimental Setup

All of the experimental data are obtained from a high intensity, backmixed, single-jet, stirred reactor as shown in Figure 1. Both fuel and air enter the reactor through the premixer. The

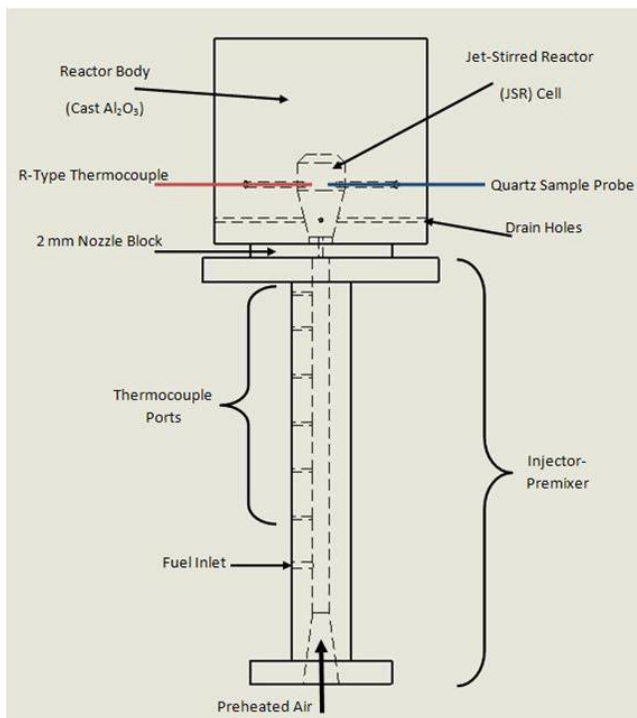

Figure 1: Diagram of Experimental Setup

air is is preheated to 573 K. Once the fuel stream is mixed with the air, the mixture has a nominal temperature of about 550 K as it enters the reactor cavity. The stagnation pressure of the premixed fuel/air mixture is measured 5 cm upstream of the reactor cavity. The premixed reactants enter the cast alumina reactor cavity through a 2mm nozzle resulting in a sonic jet velocity of approximately 450 m/s. The total volume of the reactor is a 15.8 cc, the mass flow rate of air is 1.08E-3 kg/s, and nominal combustion temperature is held constant at 1800 K. This results in a mean fluid residence time of 2.7 ± 0.2 ms.

As shown in Figure 2, both temperature and species concentrations are measured at 2/3 of the reactor height with the nominal sampling location being 2 mm inside the reactor wall.

This sampling location is far enough into the reactor to avoid thermal and fluid boundary layer effects, but not so far as to experience the effects of the jet. In addition to collecting data at the standard sampling location, detailed reactor spatial probing is conducted in order to gain insight of flame structure within the reactor. Both temperature and species measurements are taken radially between the reactor wall and centerline at 2/3 of the total reactor height.

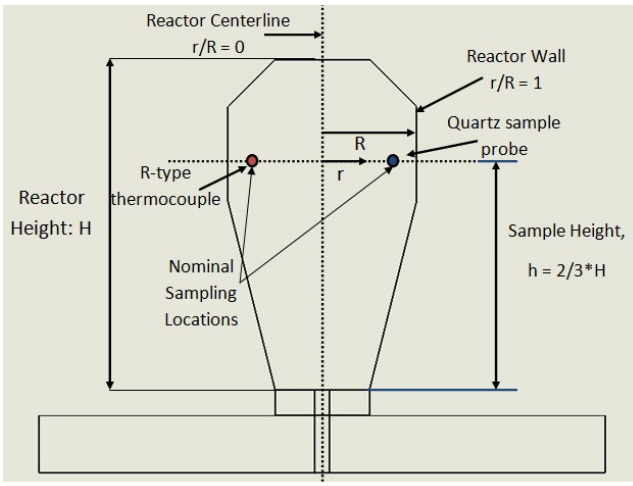

Figure 2: Sampling locations within the JSR

The combustion gas temperature is measured with a type R thermocouple that is coated with alumina to prevent catalytic effects. The measured combustion temperature is between 50 and 70 K below the reported temperature which has been corrected for both radiation to the colder reactor wall and conduction through the wire [7]. The hot combustion gases are sampled through a quartz sample probe that is cooled with warm water. The sample gas is drawn by a metal bellows pump into a heated teflon tube (to prevent condensation). The sample is then drawn through an ice bath where the H_2O in the sample is removed and the dried gas is sent to a three gas (CO_2, CO, and O_2) analyzer and a NO_X analyzer in parallel. The CO_2 and CO analyzers operate on the NDIR principle, while the O_2 and NO_X analyzers are paramagnetic and chemiluminescent instruments, respectively.

3 Experimental Results

Since the experiments focus on the influence of the diluents on NO_X, we designed the experiments to hold the temperature constant for all diluent concentrations (N_2 versus CO_2). We achieve this as follows. First, the air flow is held constant. The CH_4 flow is selected to achieve a constant temperature of 1800 K in the recirculation zone. As the diluent loading is increased, the natural tendency of the reactor to run cooler is balanced by increasing the CH_4 flow rate. Thus, as the diluent is increased, the CH_4 flow rate is also increased, and the overall fuel/oxidant ratio approaches stoichiometric.

An important question is how to best present the NO_X data. In the present experiments (1) the stoichiometry varies, and (2) the CO_2 and N_2 dilute the flow. NO_X mole fraction (as ppm) is the common way to present the emission data. The mole fraction is, however, influenced by dilution effects, in this case both due to stoichiometry and dilution. While the stoichiometry effect can be handled by correcting to a common O_2 value, the presence of the diluents can change mole fraction without any change in chemistry. We thus conclude that the most meaningful way to present the data is as a NO_X emission index, i.e. the amount of NO_X formation attributed to each unit of CH_4 entering the reactor. This avoids mole fraction changes that are due only to dilution (via variable stoichiometry or CO_2 versus N_2). Recently, ElKady et al. [3] have derived a NO_X correction to 15% O_2 that is based on an oxidizer composed of O_2, N_2, and CO_2; however, it is determined that their method is algebraically equivalent to the emission index separated by a constant. For the remainder of the document, the NO_X emissions are expressed as an emission index since it is a more common method of expressing pollutant emissions.

Figure 3 shows that the NO_X emission index (grams NO_X/kg CH_4) increases for both N_2 and CO_2 dilution. The results also show that dilution with N_2 is more effective at enhancing NO_X formation than CO_2 dilution. There are, however, several ways to correlate the effect of the diluents, e.g., plotting against mass fraction of diluent, mole fraction of diluent, etc. As mentioned above, increasing the diluent flow requires an increase in CH_4 flow to maintain the 1800 K reactor temperature. This means that the mixture approaches a stoichiometric fuel-air ratio and the O_2 concentration decreases with increasing dilution. In examining the various ways to correlate the effect of the diluents on NO_X formation, we concluded that plotting against O_2 concentration was the most fundamental approach, because the relationship between fuel, O_2, and NO_X is at the core of the chemical behavior.

Figure 4 shows the NO_X emissions index plotted against the O_2 concentration in the exhaust. As in Figure 3, the fuel stream diluted with N_2 is more effective at producing NO_X emissions than with CO_2 dilution when compared on a common O_2 basis. Thus, there is evidence to suggest that there may be a chemical kinetic explanation for this phenomenon.

For reference, the measured NO_X is displayed versus exhaust O_2 concentration in Figure 5. Note that there is some difference between Figures 4 and 5. In general, the specific heat of the two additives on a mass basis is sufficiently similar that (1) the tendency of the reactor to cool upon additive addition is nearly the same for the two, and (2) the increase in CH_4 flow needed to maintain the 1800 K flame temperature is thus similar between the two. The result is that the mole fraction values and the emission index report similar trends. The other effect that

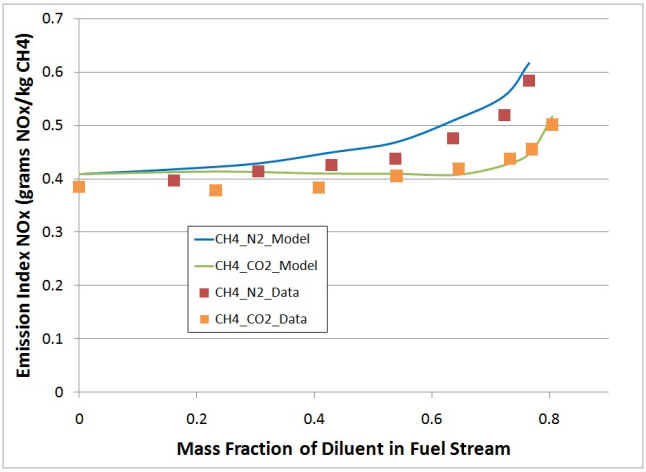

Figure 3: Measured NO_X as EI versus mass fraction of N_2 or CO_2 diluent in fuel stream. Temperature is maintained constant at 1800 K

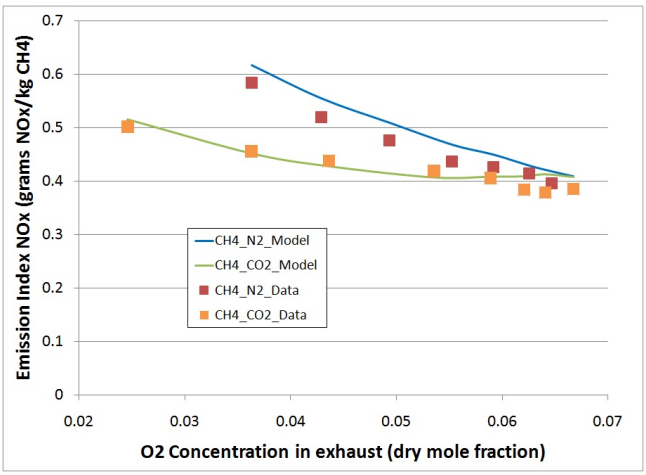

Figure 4: Measured NO_X as EI versus exit gas O_2 (mole %, dry). Temperature is maintained constant at 1800 K

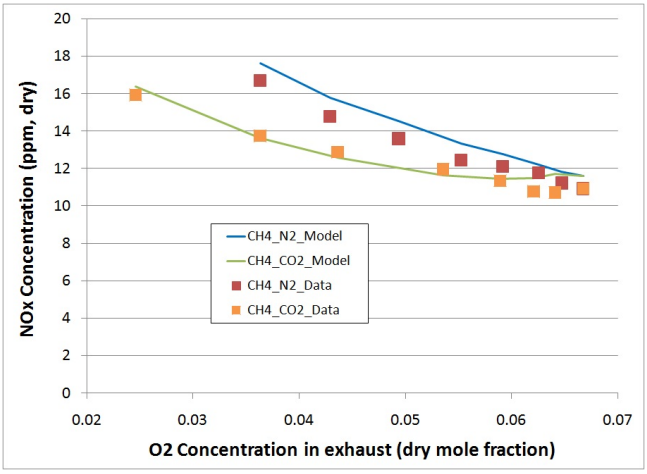

Figure 5: Measured NO_X as (ppm, dry) versus exit gas O_2 (mole %, dry). Temperature is maintained constant at 1800 K

make the data appear different on an emission index is due to the increasingly larger molecular weight in the product gas as more CO_2 is added. For N_2 dilution, the molecular weight remains essentially constant throughout the entire range of experiments. As shown in Figures 3 through 5, the model predicts the data quite well. The modelling results are discussed in more depth in Section 6.

4 CFD Modelling

Three dimensional CFD simulations are carried out with pure CH_4 premixed with air. The simulations are conducted with a domain of about 1,000,000 cells encompassing both the solid and fluid portion of the JSR. Due to the heavily swirling nature of the flow, both the standard [8] and realizable [9] k-ε models were unable to obtain convergence. Thus, the 9 equation Reynolds stress model [10] is employed due to its inherent ability to handle the highly swirling nature of the flow inside the JSR. The flow though the nozzle inlet is highly compressible; thus, density in the reactor is modelled using the ideal gas equation. A multidimensional heat transfer model is utilized that accounts for convection on both the outer and inner surfaces of the JSR, conduction within the entire domain, and radiation on both the inner and outer surface of the JSR. The radiation on the inner surface is modelled using the Discrete Ordinates Model [11], while the radiation on the outer surface is modelled as a simple black body with a view factor equal to unity. The partial differential equations that govern both flow and heat transfer within the JSR are solved using the ANSYS Fluent software package [12].

The chemistry within the reactor is modelled with the finite rate/eddy-dissipation model [13]. In this model, the reaction rate is computed by both an Arrhenius expression and an expression that incorporates turbulent effects. The turbulent mixing, or eddy-dissipation reaction rate is governed by the the large eddy mixing time scale: k/ε, while the chemical rate is generally governed by one or two global Arrhenius steps [12]. The net reaction rate is computed as the smaller of the two rates. Global CH_4 oxidation rates for atmospheric combustion from Nicol are used in the simulation [14]. The global chemistry does a reasonably good job of predicting CH_4 and CO oxidation as shown in Figures 6 and 7.

The contours of temperature and CO concentration are shown in Figure 8. This figure illustrates the two zone combustion behavior mentioned above. The highly turbulent flame zone is anchored around the nozzle, which is outlined by the region of high CO concentration. This flame zone is then followed by a super-equilibrium post flame recirculation zone, where the radicals (indicated by CO concentration) are starting to relax and the temperature is fairly uniform. Although, this CFD model does not predict intermediate radicals and NO_X, the CO contours and flow field can be used as guidelines to develop a chemical reactor network (CRN), which can incorporate detailed chemistry.

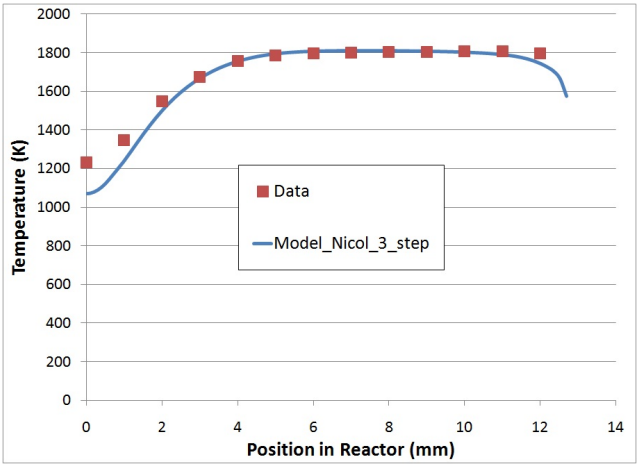

Figure 6: Profile of temperature from reactor centerline to wall, measured and predicted by CFD for CH_4 combustion (w/o diluents) for exit gas O_2 of 6.6% (mole %, dry)

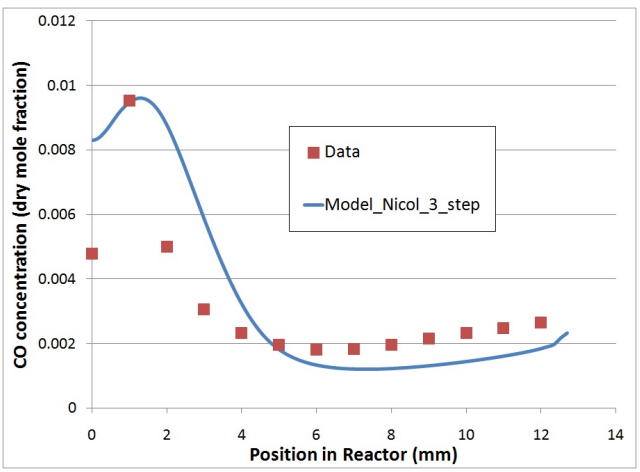

Figure 7: Profile of CO from reactor centerline to wall, measured and predicted by CFD for CH_4 combustion (w/o diluents) for exit gas O_2 of 6.6% (mole %, dry)

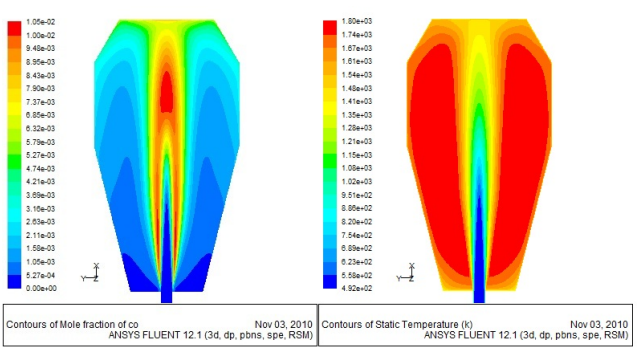

Figure 8: CO and temperature contours by CFD for JSR fired on CH_4 (w/o diluents) for exit gas O_2 of 6.6% (mole %, dry)

5 Development of the CRN

The CFD model is used as a basis to construct a chemical reactor network composed of perfectly stirred reactors (PSR) as shown in Figure 9. The first element, PSR 1, represents the turbulent flame brush surrounding the jet that does not see any entrainment from the recirculation zone. It is modelled as a PSR at blowout, which is an adiabatic PSR that is 1% larger than the smallest volume that will sustain combustion with the given inlet conditions. From the CFD model, it is found that approximately 90% of the flow leaving the jet passes through this reactor. About 10% of the flow proceeds through the side of the jet and mixes with hot gases coming from the recirculation zone. Denoted as PSR 3, or shear zone, this reactor is representative of a turbulent premixed strained flame, where cold reactants strain against hot recirculated products. PSR 3 is also adiabatic since it does not come into contact with the outside wall. Its volume is estimated to be about half of the volume computed for PSR 1 from the CFD simulation. The contents of both PSR 1 and PSR 3 continue into PSR 2, which represents the recirculation zone that contains super-equilibrium free radicals. PSR 2 is assigned the remaining reactor volume (most of the JSR volume) and is run at a non-adiabatic temperature of 1800 K. The CFD model is again consulted to choose the flow fraction that is being exhausted rather than sent back to the recirculation zone. At several axial locations along the height of the reactor the downward mass flow is integrated. By subtracting this value from the

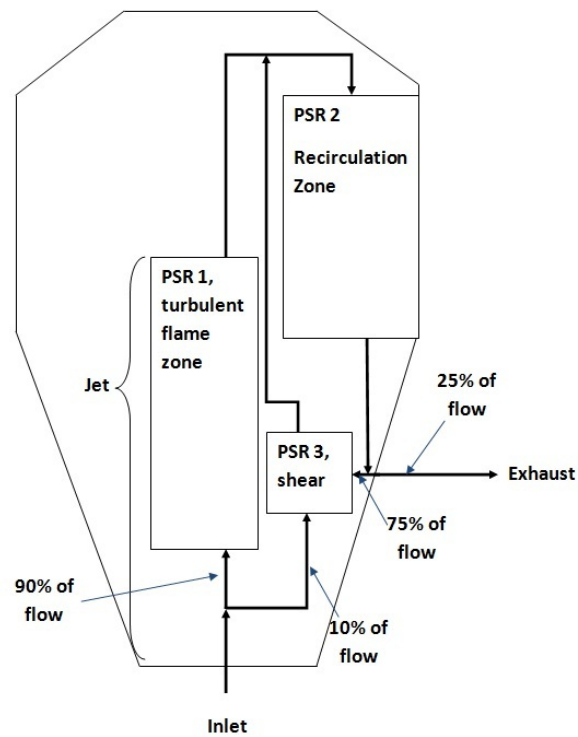

Figure 9: Chemical Reactor Network constructed with from the calculated flow field within the CFD model

known mass flow leaving the reactor (mass conservation), one obtains an estimate for the mass flow that is returning to the recirculation zone through PSR 3. This calculation indicates that approximately 75% of the flow returns to the recirculation zone, while 25% is exhausted. This flow fraction is verified by using the particle tracking feature within the software [12].

6 CRN Modelling Results and Discussion

For all of the modelling reported here, the 52 species, 323 reaction GRI 3.0 mechanism is utilized [15]. As shown in Figures 3 through 5, the model predicts the experimental NO_X data quite well.

These results raise two main questions: (1) Why do NO_X emissions go up when the O_2 in the exhaust decreases/mass fraction of diluent increases? and (2) Why are NO_X emissions higher for fuels diluted with N_2 rather than CO_2?

In order to gain a better insight on these trends, each of the four NO_X production pathways is isolated and the model is rerun. The four pathways to NO_X formation are Zeldovich [16], N_2O [17], NNH [18], and prompt [19], and the contributions of each to the total NO_X emission index is noted as a function of dilution in Figures 10 and 11. Figure 12 shows the pathway contribution within each reactor of the CRN at a common O_2 concentration of 3.6% dry mole fraction in the exhaust. Here the emission index is calculated from the NO_X rate of production within each reactor and the reactor residence time.

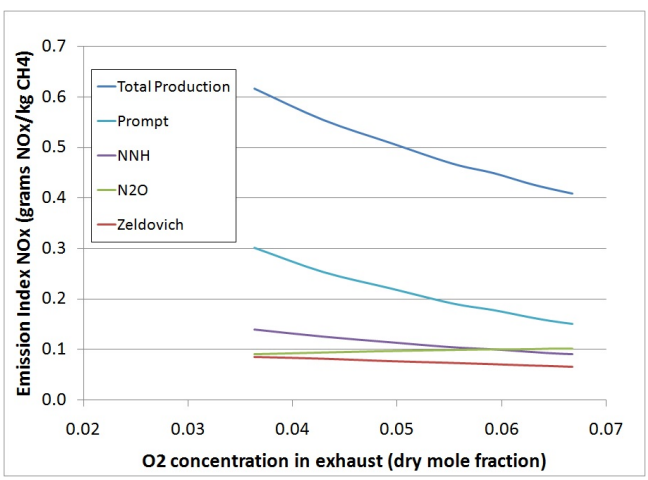

Figure 10: NO_X emission index predicted by CRN model: total and by four pathways. CH_4 diluted with N_2

There are a couple points worth noting. Due to the small volume and extremely short residence time of the shear reactor (it has approximately three times more mass flow than the flame brush), it is essentially a mixing element and can be ignored when discussing chemical effects. Thus, attention can be

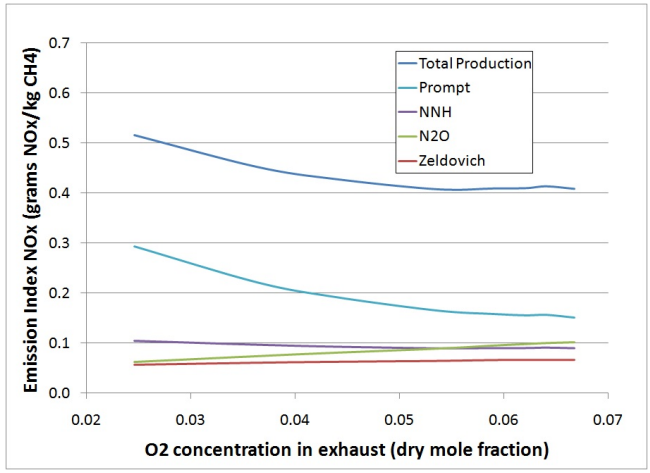

Figure 11: NO_X emission index predicted by CRN model: total and by four pathways. CH_4 diluted with CO_2

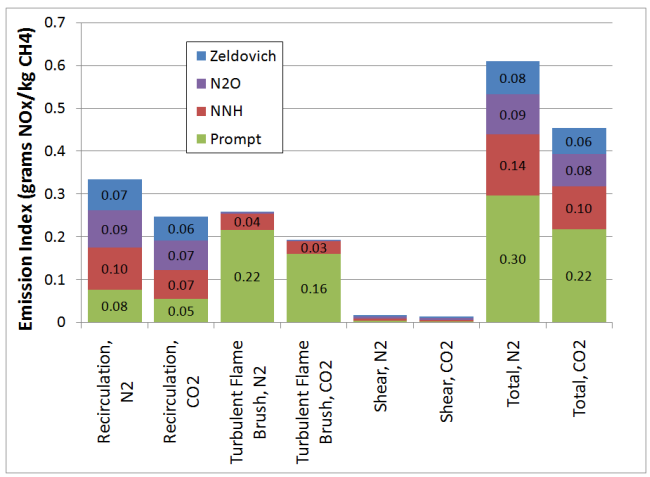

Figure 12: NO_X production reported as emission index for each of the four mechanisms in each of the three reactor elements of the CRN model. O_2 concentration is 3.6% (dry mole fraction)

focussed on the flame brush and recirculation zone. Analysis of Figures 10, 11, and 12 show the following trends for NO_X formation in the JSR:

1. Similar to the atmospheric pressure modelling work done by Li et al. [5], prompt NO_X is the major source of NO_X for this experiment, and all three figures support this.
   (a) This may be related to the relatively high CH_4-air equivalence ratios used: 0.71-0.86 for N_2 dilution and 0.71-0.92 for CO_2 dilution. Note that for most LPM combustion devices operating on CH_4, the equivalence ratio ranges from 0.45 to 0.65.
   (b) The prompt NO_X increases as the dilution level is increased (i.e. as the exit gas O_2 decreases). This is expected because of the increasing amounts of CH_4 required as the dilution levels are increased.
   (c) Much of the prompt NO_X is formed in the turbulent

flame brush (i.e. flame zone) modelled as an adiabatic PSR operating near blowout condition. The highly non-equilibrium nature of this environment may support significant prompt NO_X, even under fuel-lean conditions.

2. NNH contributes a relatively small amount of NO_X and the N_2O and Zeldovich sources of NO_X are negligible within the flame brush as shown in Figure 12, because of this reactor's short residence and low temperature. The computed temperature within the flame brush ranges between 1609 and 1612 K for both diluted fuels at all dilution levels.
3. All four sources of NO_X contribute in the recirculation zone, modelled as a PSR at measured temperature (1800 K).
4. The sources of NO_X are greater for N_2 dilution than for CO_2 dilution in both the turbulent flame brush and the recirculation zone.

These NO_X trends are supported by the concentrations of free radicals O, H, and CH shown in Figures 13, 14, and 15, as calculated from the CRN modelling.

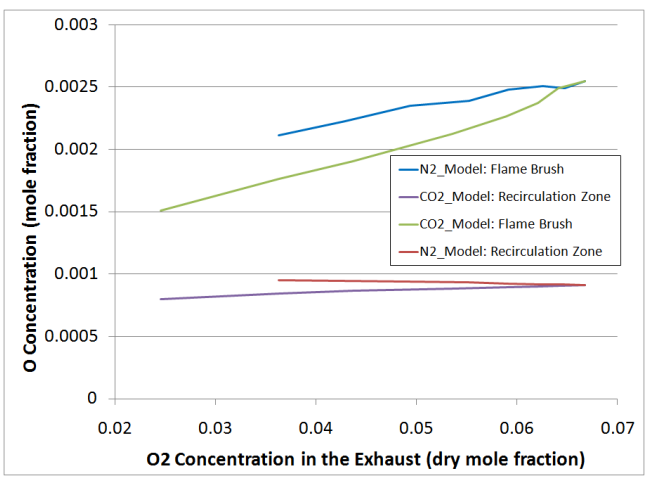

Figure 13: O atom concentration in the recirculation zone and PSB for both diluted fuels

When compared to no dilution, the N_2 mole fraction is 5% greater for maximum N_2 dilution and 17% smaller for maximum CO_2 dilution. For small concentrations of NO_X at constant temperature (which is the case here) Zeldovich NO_X forms in proportion to $[N_2][O]$, where [ ] means moles/vol. Looking at the recirculation zone, for increasing N_2 dilution, O is nearly constant and N_2 increases; thus, Zeldovich NO_X increases with dilution. However, for increasing CO_2 dilution, mole fractions of both O and N_2 decrease: thus, Zeldovich NO_X decreases with dilution.

Nitrous oxide (N_2O) is depleted by reaction with both O and H; however, in this pathway NO is only formed directly through reaction with O. As shown above in Figure 12 most of the NO_X

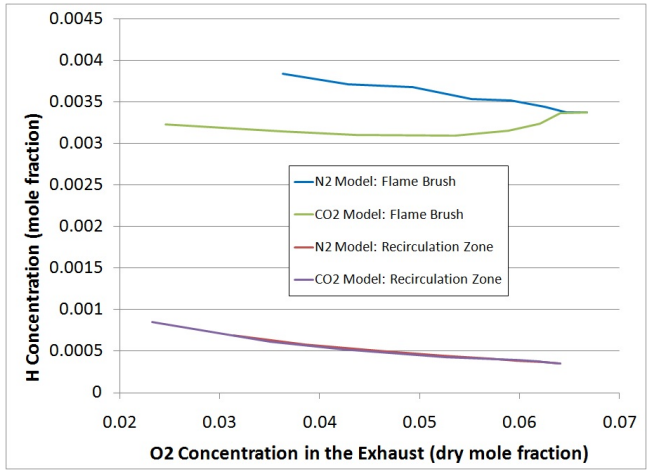

Figure 14: H-atom concentration in the recirculation zone and turbulent flame brush for both diluted fuels

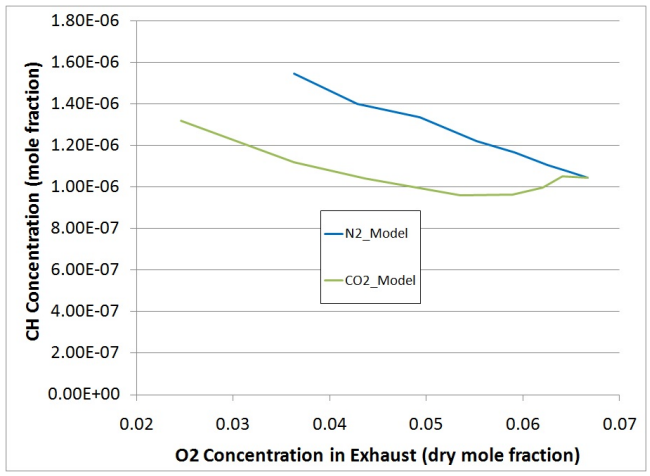

Figure 15: CH concentration within the Flame Brush for CH_4 diluted with both N_2 and CO_2

formed through the N_2O pathway is formed in the recirculation zone. Figure 14 shows H-atom increasing as the dilution level of the JSR increases. This trend is the same for both N_2 and CO_2 dilution. Shown in Figure 13, the O concentration in the recirculation zone falls slightly for CO_2 dilution and stays flat for dilution with N_2. Due to both of these effects, the contribution to NO production from N_2O falls for both diluents as dilution increases; slightly more for CO_2 dilution than N_2.

As seen in Figures 10 and 11, NO formed from NNH increases as the N_2 and CO_2 dilution levels increase. As noted from Figure 12, it forms in both reactor zones. NNH is formed by reaction of N_2 with H, and NO is formed by reaction of NNH with O. NNH concentration follows the upward trend shown for H-atom in Figure 14, tempered by increasing N_2 concentration for N_2 dilution and decreasing N_2 concentration for CO_2 dilution. The result is a somewhat greater increase in NO with dilution level for N_2 than for CO_2.

Prompt NO forms as CH radical reacts with N_2 to form HCN and N, both of which oxidize to NO. CH has a short lifetime; thus, the prompt NO is produced more significantly in the flame brush than in the recirculation zone. The flame brush concentrations of CH are plotted in Figure 15, where they are seen to increase significantly as more N_2 and CH_4 are added to the reactor. Small amounts of CO_2 dilution appear to suppress CH, though as more CO_2 is added, the CH increases.

In addition to the above analysis, both Glarborg et al. [20] and Liu et al. [21] have shown that large concentrations of CO_2 will compete with O_2 for H-atom via the reaction:

$$H + CO_2 \rightleftarrows CO + OH.$$

The consumption of H atom will decrease the rate of the most significant chain branching reaction:

$$H + O_2 \rightleftarrows OH + O.$$

This suppression effectively reduces the size of the O/H/OH radical pool, which is supported by the trends shown in Figures 13 and 14. This decrease in O and H concentration will suppress the formation of NO_X through the Zeldovich, N_2O and NNH pathways.

7 Conclusions

A recirculation-stabilized combustor is used to generate NO_X emission data for LPM CH_4/air combustion diluted with either N_2 or CO_2 at atmospheric pressure. This experiment is designed to simulate the combustion of landfill gas. The experiments are conducted at a constant reactor temperature and residence time. NO_X emissions (expressed in terms of CH_4 emissions index) increase with dilution, and dilution with N_2 yields higher NO_X emissions than dilution with CO_2. To explain these results, a chemical reactor network, CRN, is developed using insight from a three dimensional CFD simulation with simplified chemistry. This CRN with the full GRI 3.0 mechanism is shown to effectively model the experimental data collected.

The CRN model indicates that the increase in NO_X emissions with increased dilution is due to an enhancement of the prompt NO_X pathway resulting from an increase in the CH radical concentration as the mixture moves towards stoichiometric. The model also suggests that both a smaller N_2 concentration and a preferential loss of free radicals for dilution with CO_2, results in decreased NO_X emissions for CO_2 dilution vs. N_2 dilution.

These results are in agreement with other studies looking at the addition of diluent to constant temperature LPM CH_4 flames at atmospheric pressure [2], [5]. However, the literature suggests that at elevated pressures, the addition of diluent to a LPM CH_4 flame actually inhibits NO_X formation in flames at equivalent combustion temperatures.

ACKNOWLEDGMENT

Support for this project was provided by the California Energy Commission through Agreement No. 500-08-034 through the University of California-Irvine. We wish to acknowledge Marla Mueller, Technical Lead, who is the Technical Project Officer at the California Energy Commission, and Vincent McDonell, who is the Project Manager at UC Irvine.

REFERENCES

[1] Mintz, M., Han, J., Wang, M., and Saricks, C., 2010. Well-to-wheels analysis of landfill gas-based pathways and their addition to the greet model. Tech. rep., Argonne National Laboratory.

[2] Qin, W., Egolfopoulos, F. N., and Tsotsis, T. T., 2001. "Fundamental and environmental aspects of landfill gas utilization for power generation". *Chemical Engineering Journal,* **82**, pp. 157–172.

[3] ElKady, A. M., Evulet, A., Brand, A., Ursin, T. P., and Lynghjem, A., 2009. "Application of exhaust gas recirculation in a DLN F-class combustion system for postcombustion carbon capture". *Journal of Engineering for Gas Turbines and Power,* **131**.

[4] Røkke, P. E., and Hustad, J. E., 2005. "Exhaust gas recirculation in gas turbines for reduction of CO_2 emissions; combustion testing with focus on stability and emissions". *International Journal of Thermodynamics,* **8**, pp. 167–173.

[5] Li, H., ElKady, A. M., and Evulet, A. T., 2009. "Effect of exhaust gas recirculation on NO_X formation in premixed combustion system". In 47th AIAA Aerospace Sciences Meeting Including The New Horizons Forum and Aerospace Exposition.

[6] Steele, R. C., Tonouchi, J. H., Nicol, D. G., Horning, D. C., Malte, P. C., and Pratt, D. T., 1998. "Characterization of NO_X, N_2O, and CO for lean-premixed combustion in a high-pressure jet-stirred reactor". *Journal of Engineering for Gas Turbines and Power,* **120**, pp. 303–310.

[7] Steele, R. C., 1995. "NO_X and N_2O formation in lean-premixed jet-stirred reactors operated from 1 to 7 atm". PhD thesis, University of Washington.

[8] Launder, B. E., and Spalding, D. B., 1972. *Lectures in Mathematical Models of Turbulence*. Lectures in Mathematical Models of Turbulence.

[9] Shih, T. H., Liou, W. W., Shabbir, A., Yang, Z., and Zhu, J., 1995. "A new k-ε eddy-viscosity model for high reynolds number turbulent flows - model development and validation.". *Computers Fluids,* **24**, pp. 227–238.

[10] Launder, B. E., 1989. "Second-moment closure: Present...

and future?". *International Journal of of Heat and Fluid Flow,* **10**, pp. 282–300.

[11] Raithby, G. D., and Chui, E. H., 1990. "A finite-volume method for predicting a radiant heat transfer in enclosures with participating media". *Journal of Heat Transfer,* **112**, pp. 415–423.

[12] *ANSYS Fluent, Academic Research, Release 12.0*.

[13] Magnussen, B. F., and Hjertager, B. H., 1976. "On mathematical models of turbulent combustion with special emphasis on soot formation and combustion". In Proceedings of the 16th International Symposium on Combustion, The Combustion Institute.

[14] Nicol, D. G., Malte, P. C., Hamer, A. J., Roby, R. J., and Steele, R. C., 1998. "Development of a five-step global methane oxidation-NO formation mechanism for lean-premixed gas turbine combustion". In Proceedings of the International Gas Turbine and Aeroengine Congress and Exhibition: Stockholm, Sweden.

[15] Grimech3.0. http://www.me.berkeley.edu/gri mech/.

[16] Zeldovich, Y. B., 1946. "The oxidation of nitrogen in combustion and explosions". *Acta Physicochemica USSR,* **21**, pp. 577–628.

[17] Malte, P. C., and Pratt, D. T., 1974. "The role of energy-realeasing kinetics in NO_X formation: Fuel-lean, jet-stirred CO-air combustion". *Combustion Science and Technology,* **9**, pp. 221–231.

[18] Bozzelli, J. W., and Dean, A. M., 1995. "O + NNH: A possible new route for NO_X formation in flames". *International Journal of Chemical Kinetics,* **27**, pp. 1097–1109.

[19] Fenimore, C. P., 1971. "Formation of nitric oxide in premixed hydrocarbon flames". In Thirteenth Symposium (International) on Combustion, The Combustion Institute.

[20] Glarborg, P., and Bentzen, L. L. B., 2008. "Chemical effects of a high CO_2 concentration in oxy-fuel combustion of methane". *Energy & Fuels,* **22**, pp. 291–296.

[21] Liu, F., Guo, H., and Smallwood, G. J., 2003. "The chemical effect of CO_2 replacement of N_2 in air on the burning velocity of CH_4 and H_2 premixed flames". *Combustion and Flame,* **133**, pp. 495–497.